Journal of Alloys and Compounds 271–273 (1998) 831–836

Optical and magneto-optical spectroscopy of uranium and plutonium compounds: recent theoretical progress

P.M. Oppeneer[a,*], A.Ya. Perlov[1,a], V.N. Antonov[1,a], A.N. Yaresko[1,a], T. Kraft[a], M.S.S. Brooks[b]

[a] *Max-Planck Research Group 'Theory of Complex and Correlated Electron Systems', University of Technology, D-01062 Dresden, Germany*
[b] *European Commission, Joint Research Center, Institute for Transuranium Elements, D-76125 Karlsruhe, Germany*

Abstract

First-principles calculations are reported which illustrate that, for those actinide compounds where the 5f electrons are sufficiently delocalized, energy band theory based upon the local spin-density approximation (LSDA) describes the optical and MO spectra reasonably well. Examples which we examine in detail are URhAl and UFe_2. The delocalized LSDA approach meets limitations for those actinide compounds, where the electrons in the correlated 5f shell are nearly localized. Just as in the case of lanthanide compounds having localized 4f electrons, a satisfactory description of the optical spectra could be obtained by using a generalization of the LSDA, in which explicitly f electron Coulomb correlations are taken into account (LSDA+U approach). A third group consists of compounds in which the 5f electrons are neither fully delocalized nor localized, but have experimentally been classified as quasilocalized. The suitable theoretical approach to such compounds is yet to be resolved. We further consider the Pu monochalcogenides, the unusual physical properties of which were previously treated with different models, and discuss the optical spectrum of PuTe. © 1998 Elsevier Science S.A.

Keywords: First-principles calculations; Actinide; URhAl; UFe_2; PuTe; Optical spectrum

1. Introduction

One of the most intriguing aspects of actinide compounds is the great variability in the localization degree of the 5f electrons. Varying from one actinide compound to another, the 5f electrons may range from being nearly localized to being practically itinerant. The 5f localization tendency and concomitant physical properties have been extensively investigated for uranium intermetallic compounds (see, e.g. Refs. [1,2]). The 5f localization tendency may be looked upon in terms of the 5f band width, which is narrower than the 3d band width, yet broader than that of 4f [3]. These two enveloping bounds mark the different approaches to treating the 5f electrons that have become customary: either a model of localized f electrons is adopted, which has proven to be applicable to explaining many properties of lanthanides, or a delocalized band model is adopted. The latter has proven to be the valid approach for transition metals.

If we now consider the group of U intermetallics in more detail, and see how many compounds have actually been classified as having localized 5f electrons, then it appears that only a few compounds could be classified as such. The clearest example is UPd_3, where experimentally the 5f electrons were detected at 1 eV below the Fermi energy (E_F) [4], and a sharp crystal field (CF) transition was observed [5]. The latter is, in analogy to the CF transitions in lanthanides, a fingerprint of localized f electrons. Very recently, an inelastic neutron peak was observed for URhAl, which could be due to an intermultiplet transition [6]. This observation thus raises the interesting question if URhAl could possibly be a localized f material. For quite a number of other U compounds it has been found that the 5f electrons are not really localized, neither are they fully delocalized. This sort of intermediate case has been termed 'semilocalized' or 'quasilocalized'. An experimental definition for semilocalized 5f electrons is that the occupied 5f electrons are detected at 0.5–0.8 eV below E_F. This is found to be the case for, e.g. USe [7], UTe [8], and UNiSn and UPtSn [9]. In various other U compounds the 5f electrons are considered to be delocalized. Well-known examples are UN [10] and UFe_2 [11]. This (de)localization classification is somewhat simplified, because the origin of 5f delocalization (due to direct f–f overlap or f ligand hybridization) is not considered.

---

[*] Corresponding author. Tel.: +49 351 4634282; fax: +49 351 4637029; e-mail: peter@tmps08.mpg.tu-dresden.de

[1] Permanent address: Institute of Metal Physics, Academy of Sciences of Ukraine, 252680 Kiev, Ukraine.

PII: S0925-8388(98)00228-X

Optical spectroscopy provides a powerful, widely used tool to investigate in much detail the electronic structure of lanthanides and actinides. Traditionally, one distinguishes the various existing kinds of spectroscopies according to the photon energy of the employed light, i.e. high-energy X-ray methods, and methods applying infrared, visible or medium-energy light ($\hbar\omega < 10$ eV). X-ray photoemission spectroscopy (XPS) has been applied to determine the energy position of the 5f states below E_F, and angle-resolved XPS has been used to map out the energy bands in the Brillouin zone (see, e.g. Ref. [12]). Optical spectroscopy in the visible and infrared energy range has successfully been applied to many topics in lanthanide and actinide research. Examples are the infrared absorption in the heavy-fermion state of URu_2Si_2 [13] and UPd_2Al_3 [14], reflectivity spectroscopy on intermediate valence and dense Kondo materials [15]. A particularly useful spectroscopic technique is MO Kerr spectroscopy [16]. Reflectivity spectroscopy can be used to determine relative energy level positions, but Kerr spectroscopy has the additional advantage that it couples to both the spin and orbital polarization of the electron states [16]. Kerr spectroscopy is therefore ideally suited for studying magnetic actinide compounds. In the last decade numerous MO Kerr spectra of lanthanide and actinide compounds have been measured [16]. Very recently, spectacular new results have been achieved with this technique, as the discovery of a record Kerr angle of 90° in CeSb [17], and the observation of a magnetically polarized, empty $4f^1$ level in LaSe [18]. It can be anticipated that other important discoveries will be reported in the future.

Many valuable experimental spectroscopic data were obtained in the last two decades, yet the first-principles theory of MO spectra was only starting to be developed a few years ago [19,20]. Within the current theoretical progress, it has become evident that band theory on the basis of the local spin-density approximation (LSDA) provides a minute description of the optical and MO Kerr spectra of most transition-metal compounds [21]. In the case of actinide intermetallics, theoretical studies of their spectra are still rare, the research field is thus only in its infancy. One important conclusion, which has so far been reached, is that an appropriate description of the electronic structure (including degree of f localization) will provide an accurate explanation of the measured spectra. Precisely this feature is of great help in deciding if an actinide intermetallic can be regarded as having delocalized 5f electrons or not.

2. Computational formalism

For a detailed account of the theoretical formalism we refer to Ref. [19]. We mention here that we employ the linear response method to evaluate the full optical conductivity tensor, $\sigma_{ij}(\omega)$. Other spectroscopic quantities, such as the reflectivity or MO Kerr spectrum can directly be derived from σ_{ij} [16]. The Kerr rotation θ_K and Kerr ellipticity ε_K, e.g. are in the polar geometry (i.e. magnetization in z-direction) given by

$$\theta_K(\omega) + i\epsilon_K(\omega) \approx -\sigma_{xy}\left[\sigma_{xx}\left(1 + \frac{4\pi i}{\omega}\sigma_{xx}\right)^{1/2}\right]^{-1}. \quad (1)$$

There are two distinct contributions to the diagonal conductivity σ_{ii} known, the so-called interband and intraband contributions. The intraband contribution is due to electron relaxation processes at E_F, therefore it plays a role at small photon energies. It can be written in the form of a Drude-type conductivity. The interband contribution stems from all optically allowed energy band transitions. To compute σ_{ij}, the state energies and wave functions are required, which we have computed using the relativistic ASW and LMTO bandstructure methods [22,23]. For broad band materials, the band energies are accurately given by the LSDA approach [24]. If, however, strong on-site Coulomb correlations are present, the LSDA does not suffice any longer. A simple correction of the LSDA is to add 'by hand' a Hubbard-like on-site f Coulomb correlation term to the LSDA Hamiltonian, for which reason this approach is called LSDA$+U$ [25,26].

In the following we will direct our attention to several representative materials. The U compounds that we consider here are URhAl and UFe_2. Since there are no MO spectra available for a U compound which exhibits truly localized f behavior, we shall consider the lanthanide compound CeBi, which has a localized 4f level. In addition we investigate the Pu monochalcogenides, which have drawn attention recently.

3. Localized f electrons: the case of CeBi

The Ce monopnictides and chalcogenides display many unusual properties (see, e.g. Refs. [27–29]). The Ce monopnictides are categorized as low-carrier dense Kondo systems [28,29]. In common with the Ce monochalcogenides, they exhibit localized 4f behavior. The only exception is CeN, which was previously classified to be a typical mixed valence material [30]. Very recently, however, first-principles LSDA calculations of the diagonal optical conductivity σ_{xx} demonstrated that the more appropriate picture of CeN is evidently that of a 4f-band material [31]. In contrast to CeN, it has recently been shown for CeSe, CeTe, and CeSb that not the LSDA, but the LSDA$+U$ approach yields the appropriate description of the optical and MO Kerr spectra [32,33]. In these Ce compounds there is one $4f^1$ level at 2–4 eV below E_F [34].

The MO Kerr spectrum of CeBi is of considerable interest, because for CeSb the exciting discovery of a record Kerr angle of 90° was very recently reported [17]. An angle of 90° is the absolute maximum value that can be measured. It is two orders of magnitude larger than the values that are commonly measured for transition-metal compounds, and about one order of magnitude larger than values maximally achieved for other lanthanide and actinide compounds [16]. The source of the MO Kerr effect is simultaneous spin and orbital polarization, whereby time reversal symmetry is broken. In most compounds the magnitude of the Kerr effect is proportional to the spin-orbit (SO) coupling interaction [35]. The MO Kerr effect in MnBi is, for example, larger than that in MnSb, because the SO coupling on Bi is larger than that on Sb [36]. One could thus expect that the Kerr angle in CeBi should be as large as, or even larger than, that of CeSb. However, this is not found to be the case [37]. In Fig. 1 we show the experimental [37] and theoretical Kerr spectrum of CeBi. The measured maximal Kerr rotation amounts only to $-9°$, ten times less than that of CeSb. The LSDA+U approach (with $U=6$ eV) explains the measured MO Kerr spectrum of CeBi fairly well. There is a small energy difference of 0.1 eV in the position of the rotation maximum, and the calculated Kerr ellipticity deviates above 0.5 eV from the experimental curve.

The fact that the Kerr rotation of CeBi is far less than that of CeSb is fully reproduced by our calculations [32,33], but it is not consistent with our experience that the Kerr effect is proportional to the magnitude of SO coupling. This suggests that the anomalously large Kerr rotation in CeSb has a different origin. Recently we have shown that there are two major contributions to the record Kerr effect in CeSb [32]: first, the denominator of Eq. (1), i.e.

$$\sigma_{xx}\left(1+\frac{4\pi i}{\omega}\sigma_{xx}\right)^{1/2},$$

becomes very small for $\hbar\omega\approx 0.4$ eV and, second, due to the strong Coulomb repulsion, an asymmetric, spin and orbitally polarized $4f^1$ level is formed. Only one chirality kind of circularly polarized light can couple to this $4f^1$ level. Yet, calculations showed that the symmetry broken coupling of circularly polarized light to the $4f^1$ level itself is not responsible for the record Kerr rotation. Rather, due to interaction of the Sb p states with the anisotropic $4f^1$ level, these become also anisotropically polarized [32,33], i.e. anisotropic p–f mixing occurs [23]. The latter results in a relatively large off-diagonal conductivity σ_{xy} for optical transitions from the anisotropic Sb p states. The imaginary part of σ_{xy} is for CeBi as large as that of CeSb, but if we compare the σ_{xx} of CeBi to that of CeSb, then we find that the denominator does not become as small for CeBi. The resulting Kerr angle of CeBi is therefore not as large as that of CeSb. We conclude that LSDA+U approach provides an improved electronic structure for materials having deep-lying, nearly localized f electrons. The optical and MO spectra computed therefrom are in fair accord with experimental spectra. The overall agreement of the calculated and experimental spectra, however, emphasizes that improvements are still called for.

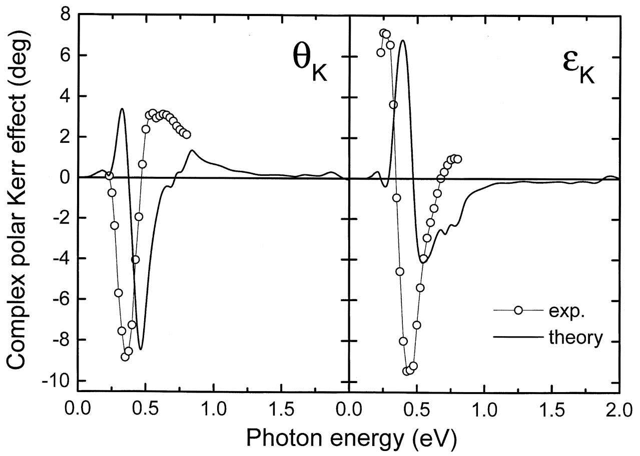

Fig. 1. Theoretical and experimental [37] Kerr angle (θ_K) and Kerr ellipticity (ϵ_K) spectrum of CeBi. The theoretical spectrum (solid curve) has been calculated using the LSDA+U approach with $U=6$ eV.

4. Uranium compounds URhAl and UFe_2

Inelastic neutron scattering experiments on URhAl revealed a peak at 380 meV, which could be the signature of an intermultiplet transition [6]. The value of 380 meV is quite close to the intermultiplet transition energy of 390 meV measured for UPd_3 [5]. There are, however, several other properties of URhAl that would advocate rather delocalized 5f behavior in URhAl. A small U moment of only 0.94 μ_B was measured which corresponds to the magnetic moment of neither a $5f^2$ nor a $5f^3$ configuration [38]. A significant amount of anisotropic 5f ligand hybridization was reported [39]. Also, the measured specific heat $\gamma=60$ mJ mol^{-1} K^{-2} is not particularly small [40]. These contradictory observations demonstrate that the 5f behavior in URhAl is not yet understood.

In Fig. 2 we show the experimental Kerr spectrum [41] of URhAl together with the theoretical spectrum calculated using the itinerant LSDA approach. The first spectral peak at 1 eV, and the second one at 2–3 eV in the Kerr angle are definitely reproduced in the theoretical spectrum. The theoretical Kerr rotation drops off between 4 and 5 eV, but it is not yet clear if this also occurs in the experimental θ_K spectrum. It can, nevertheless, be concluded that the itinerant 5f model explains the measured Kerr spectrum fairly well. Clearly, this supports the picture of delocalized 5f electrons in URhAl. The calculated electronic specific heat coefficient, $\gamma=41$ mJ mol^{-1} K^{-2}, is quite reasonable since a many-body enhancement of 1.5 can be considered to be normal. The U magnetic moment is calculated to be -1.2 and 1.6 μ_B, for spin and orbital moment, respectively, whereas the measured counterparts are -1.16 and 2.10 μ_B [38]. These values indicate that the orbital polarization

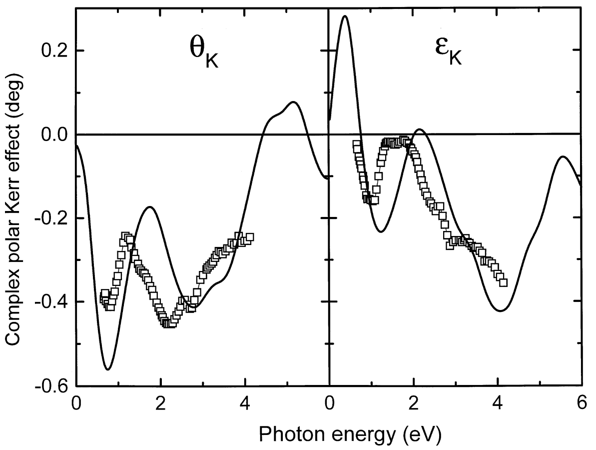

Fig. 2. Experimental [41] and theoretical Kerr spectrum of URhAl. The theoretical spectrum is calculated with the itinerant LSDA approach.

(OP) of URhAl is underestimated within the LSDA. In the last years it has become evident that one of the shortcomings of the LSDA in describing actinides is the underestimation of the OP [3]. Interestingly, the fact that the OP is too small within the LSDA does not prohibit a reasonable explanation of the MO Kerr spectrum. The same conclusion was previously also reached for UAsSe [43].

With respect to the signified intermultiplet transition, it could be speculated that the 5f electrons in URhAl divide into two groups, relatively delocalized, rather hybridized 5f electrons in the U–Rh plane, and more localized 5f electrons perpendicular to this plane, in accord with the observation of anisotropic f hybridization in URhAl [39]. The possible intermultiplet transition might correspond to the localized 5f electrons, whereas Kerr spectroscopy in the polar geometry probes the MO response in the U–Rh plane. A similar proposal has been put forward to explain the 5f behavior in UAsSe [42,43], and it has also been suggested for UPd_2Al_3 [44].

UFe_2 is one of the cubic actinide Laves phase compounds that has been intensively studied (cf. Refs. [45,46]). The general picture that has emerged for UFe_2 is that of delocalized 5f electrons which strongly hybridize with Fe 3d electrons [11,45]. As a consequence, the spin moment on U is substantially reduced from its free ion value to -0.22 μ_B, and the orbital moment to 0.23 μ_B [47]. The total moment on Fe is reduced to 0.60 μ_B [47]. Even though the delocalized 5f behavior of UFe_2 is firmly established, and though the LSDA approach does predict the correct trend in UFe_2, it has not been able to explain quantitatively the vanishing moment on U [11]. The inclusion of the OP correction brings the calculated total U moment to -0.15 μ_B [48], in better agreement with experiment. The total moment per formula unit becomes, however, 1.63 μ_B [48], which is larger than the computed total moment without OP of 1.40 μ_B and also larger than the experimental total moment of 1.19 μ_B [47].

These findings illustrate that not everything about the electronic structure of UFe_2 is explained. Another stringent test for the applicability of the LSDA approach to UFe_2 would be the description of the MO Kerr spectrum. In Fig. 3 we show the theoretical MO Kerr spectrum, calculated using the LSDA approach, for both the (001) and (111) orientations of the magnetic moments. The MO Kerr spectrum of single-crystalline UFe_2 has not yet been measured [49], i.e. the spectrum shown is a prediction. In Fig. 3 we have included the MO Kerr spectrum of Fe. It turns out that the Kerr spectrum predicted for UFe_2 is not so different from that of bcc Fe. One of the reasons for this is that the moment on U is small, i.e. direct optical transitions on U will not contribute much to the spectrum. Pilot calculations which we performed, have shown that U contributes indirectly to the Kerr spectrum through its large SO coupling contained in the hybridized, spin-polarized U–Fe bands. The magnetocrystalline anisotropy in the Kerr spectrum of UFe_2, furthermore, is calculated to be quite small. This is related to the cubic crystal symmetry and, possibly, also to the small U moment again. Experimentally the (111) axis is known to be the easy magnetization axis [45]. Our calculations for UFe_2 indeed confirm the total energy for the (111) orientation to be lower than that of the (001) orientation. We mention that we have not taken the small rhombohedral lattice distortion which is known to occur in UFe_2 into account in the calculations. We can thus confirm that the itinerant 5f treatment does correctly explain many physical properties of UFe_2. More detailed information about the electronic structure could expectedly be gained from the comparison of calculated and experimental spectra. We do, therefore,

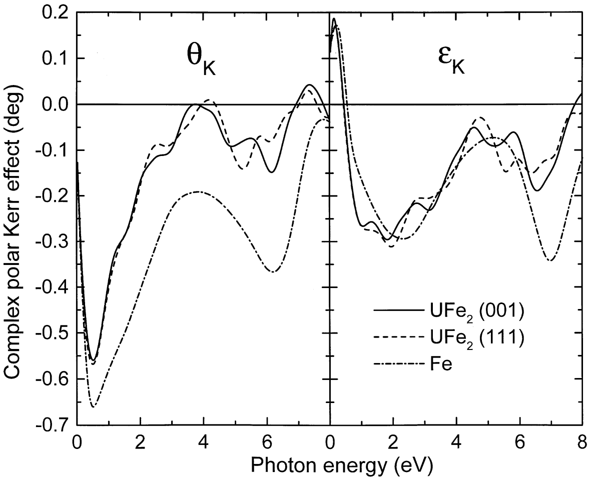

Fig. 3. Theoretical, intraband only, Kerr spectrum of UFe_2 for the (001) and (111) orientation of the magnetization. For comparison, the Kerr spectrum of bcc Fe is also shown. All spectra have been calculated with the itinerant LSDA approach.

highly encourage measurements of the optical and MO spectra of single-crystalline UFe_2.

5. The Pu-monochalcogenides

The Pu monochalcogenides are interesting materials, which display several anomalous properties [50–52]. They are temperature-independent paramagnets, exhibiting a complex semiconducting behavior. The specific heat is, at 30 mJ mol^{-1} K^{-2}, high for a semiconductor [53]. To explain these properties it was proposed that PuTe is an intermediate valent material, i.e. comparable to the collapsed phase of SmS [51]. A theoretical study proposed the Pu monochalcogenides to be relativistic semiconductors [54]. With regard to the complex semiconducting behavior, *three* different band gaps are being discussed in the literature: one large, high-temperature gap of about 0.2 eV [53], a low-temperature gap of about 20 meV [50], and even an ultra-small low-temperature gap of less than 3 meV [50,51]. The proposed electronic structure models do explain some features, but further investigations are certainly needed to obtain a complete understanding of all properties.

We have studied various properties of the Pu monochalcogenides using the LSDA approach. It is, of course, not before hand apparent that the LSDA model is applicable. Yet, our calculations show that a number of properties can be explained thereby. For example, the experimental lattice constant of PuTe is reproduced, and also the lattice constant at which the transition from the intermediate valent state to a $5f^6 6d^0$ configuration (i.e. Pu^{2+}) occurs. Calculations of the optical conductivity spectrum reveal that an optical quasigap of nearly 20 meV is predicted. In addition there is a relativistic splitting of the 5f electrons ($j=5/2$ and $j=7/2$) which apparently relates to the high temperature gap [43]. The extremely small gap of less than 3 meV is not reproduced in our single-particle calculations. We anticipate this gap to be due to quasiparticle effects.

A full account of the obtained results will be given elsewhere. We concentrate here on the reflectivity spectrum of PuTe, which was measured recently [52]. In Fig. 4 we show the experimental [52] and calculated reflectivity of PuTe. The theoretical reflectivity has been calculated using the LSDA approach, for two lattice constants, $a=6.38$ Å and $a=6.19$ Å. The latter is the experimental lattice constant, but the reflectivity spectrum for $a=6.38$ Å is found to describe the experimental data excellently. The reason for this can be traced back to a slight overestimation of the 5f, 6d hybridization in the LSDA approach. Features of the bandstructure near E_F are especially sensitive to the 5f, 6d hybridization, which varies with the lattice spacing.

On account of the calculated reflectivity, as well as other properties of PuTe, we can thus conclude that the LSDA model works reasonably well for PuTe. The picture of the electronic structure that consequently emerges from our calculations, is that of a $5f^6$ configuration having a small hybridization with the 5d states that are nearly unoccupied. Such an occupation situation resembles mostly that of the intermediate valent model [51], which does appear to be a valuable way of treating PuTe.

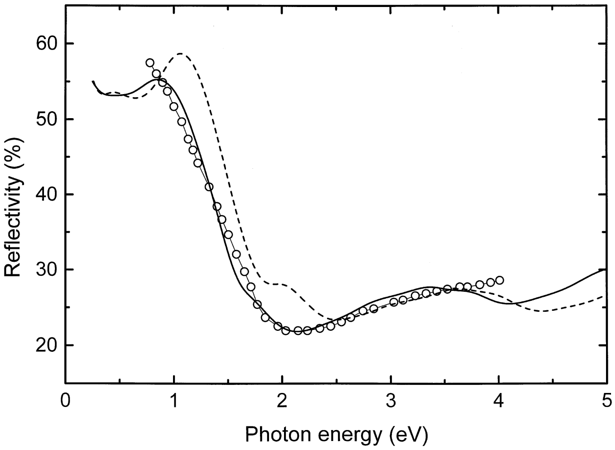

Fig. 4. Calculated and experimental reflectivity of PuTe. The experimental data (○) are after Mendik et al. [51]. The theoretical spectra are obtained using the LSDA approach, for $a=6.19$ Å (dashed curve), and $a=6.38$ Å (solid curve).

6. Summary

Recent progress in first-principles calculations of optical spectra illustrates that optical and MO spectra are developing into a powerful tool for tracing the electronic structure of lanthanide and actinide compounds. Both spectra depend quite sensitively on the underlying electronic structure, therefore these spectra can be utilized to assess the degree of localization of the f electrons. The basic notion which is extremely helpful in this respect, is that the proper electronic structure model will lead to the correct spectra (cf. Ref. [31]). For materials with deep-lying, localized f electrons the LSDA + U approach is found to reproduce the gross features of the experimental spectra [32,55], whereas the spectra of delocalized f systems are reasonably well described by the LSDA approach [31,43]. For those U compounds which have been classified to have semilocalized 5f electrons the situation needs still to be clarified. For the U monochalcogenides, which are considered to be semilocalized 5f materials [7,8], we have recently shown that the LSDA + U approach [33], assuming a $5f^2$ configuration, describes their MO Kerr spectra better than the LSDA [56,57]. Actinides exhibiting intermediate valent behavior, lastly, appear to form a separate class for which LSDA is not yet able to make a significant contribution.

However, first results obtained for PuTe indicate that the LSDA approach might be restrictedly valid.

Acknowledgements

We gratefully acknowledge valuable discussions with J. Schoenes, R. Pittini, L. Havela, V. Sechovský, M. Kučera, P. Beránková, A. Delin, and O. Eriksson.

References

[1] E. Holland-Moritz, G.H. Lander, in: K.A. Gschneidner Jr., L. Eyring, G.H. Lander, G.R. Choppin (Eds.), Handbook on the Physics and Chemistry of Rare Earths, vol. 19, North-Holland, Amsterdam, 1994, p. 1.

[2] V. Sechovský, L. Havela, in: E.P. Wohlfarth, K.H.J. Buschow (Eds.), Ferromagnetic Materials, vol. 4, North-Holland, Amsterdam, 1988, p. 309.

[3] M.S.S. Brooks, B. Johansson, in: K.H.J. Buschow (Ed.), Handbook of Magnetic Materials, vol. 7, North-Holland, Amsterdam, 1993, p. 139.

[4] Y. Baer, H.R. Ott, K. Andres, Solid State Commun. 36 (1980) 387.

[5] K.A. McEwen, U. Steigenberger, J.L. Martinez, Physica B 186–188 (1993) 670.

[6] A. Hiess, L. Havela, K. Prokeš, R.S. Eccleston, G.H. Lander, Physica B 230–232 (1997) 89.

[7] B. Reihl, N. Mårtensson, O. Vogt, J. Appl. Phys. 53 (1982) 2008.

[8] B. Reihl, N. Mårtensson, P. Heimann, D.E. Eastman, O. Vogt, Phys. Rev. Lett. 46 (1981) 1490.

[9] H. Höchst, K. Tan, K.H.J. Buschow, J. Magn. Magn. Mater. 54–57 (1986) 545.

[10] B. Reihl, G. Hollinger, F.J. Himpsel, J. Magn. Magn. Mater. 29 (1982) 303.

[11] M.S.S. Brooks, O. Eriksson, B. Johansson, J.J.M. Franse, P.H. Frings, J. Phys. F 18 (1988) L33.

[12] H. Kumigashira, S.-H. Yang, T. Yokoya, A. Chaiani, T. Takahashi, A. Uesawa, T. Suzuki, O. Sakai, Y. Kaneta, Phys. Rev. B 54 (1996) 9341.

[13] D.A. Bonn, J.D. Garrett, T. Timusk, Phys. Rev. Lett. 61 (1988) 1305.

[14] L. Degiorgi, M. Dressel, G. Grüner, N. Sato, T. Komatsubara, Europhys. Lett. 25 (1994) 311.

[15] P. Wachter, in: K.A. Gschneidner Jr., L. Eyring, G.H. Lander, G.R. Choppin (Eds.), Handbook on the Physics and Chemistry of the Rare Earths, vol. 19, North-Holland, Amsterdam, 1994, p. 177.

[16] W. Reim, J. Schoenes, in: K.H.J. Buschow, E.P. Wohlfarth (Eds.), Ferromagnetic Materials, vol. 5, North-Holland, Amsterdam, 1990, p. 133.

[17] R. Pittini, J. Schoenes, O. Vogt, P. Wachter, Phys. Rev. Lett. 77 (1996) 944.

[18] R. Pittini, J. Schoenes, F. Hulliger, P. Wachter, Phys. Rev. Lett. 78 (1997) 725.

[19] P.M. Oppeneer, T. Maurer, J. Sticht, J. Kübler, Phys. Rev. B 45 (1992) 10924.

[20] B.R. Cooper, Q.G. Sheng, S.P. Lim, C. Sanchez-Castro, N. Kioussis, J.M. Wills, J. Magn. Magn. Mater. 108 (1992) 10.

[21] P.M. Oppeneer, V.N. Antonov, in: H. Ebert, G. Schütz (Eds.), Spin-Orbit-Influenced Spectroscopies of Magnetic Solids, Springer, Berlin, 1996, p. 29.

[22] A.R. Williams, J. Kübler, C.D. Gelatt, Phys. Rev. B 19 (1979) 6094.

[23] O.K. Andersen, Phys. Rev. B 12 (1975) 3060; V.V. Nemoshkalenko, A.E. Krasovskii, V.N. Antonov, Vl.N. Antonov, U. Fleck, H. Wonn, P. Ziesche, Phys. Status Solidi (b) 120 (1983) 283.

[24] U. von Barth, L.A. Hedin, J. Phys. C 5 (1972) 1692.

[25] B.H. Brandow, Adv. Phys. 26 (1977) 651.

[26] V.I. Anisimov, J. Zaanen, O.K. Andersen, Phys. Rev. B 44 (1991) 943.

[27] H. Takahashi, T. Kasuya, J. Phys. C 18 (1985) 2697.

[28] T. Kasuya, O. Sakai, H. Harima, M. Ikeda, J. Magn. Magn. Mater. 76–77 (1988) 46.

[29] T. Suzuki, Jpn. J. Appl. Phys. Ser. 8 (1993) 267. H. Kumigashira, S.-H. Yang, T. Yokoya, A. Chaiani, T. Takahashi, A. Uesawa, T. Suzuki, Phys. Rev. B 55 (1997) R3355.

[30] Y. Baer, C. Zürcher, Phys. Rev. Lett. 39 (1977) 956.

[31] A. Delin, P.M. Oppeneer, M.S.S. Brooks, T. Kraft, B. Johansson, O. Eriksson, Phys. Rev. B 55 (1997) R10173.

[32] A.N. Yaresko, P.M. Oppeneer, A.Y. Perlov, V.N. Antonov, T. Kraft, H. Eschrig, Europhys. Lett. 36 (1996) 551.

[33] P.M. Oppeneer, V.N. Antonov, A.Ya. Perlov, A.N. Yaresko, T. Kraft, H. Eschrig, Physica B 230–232 (1997) 544.

[34] A. Franciosi, J.H. Weaver, N. Mårtensson, M. Croft, Phys. Rev. B 24 (1981) 3651.

[35] P.M. Oppeneer, J. Sticht, T. Maurer, J. Kübler, Z. Phys. B 88 (1992) 309.

[36] P.M. Oppeneer, V.N. Antonov, T. Kraft, H. Eschrig, A.N. Yaresko, A.Ya. Perlov, J. Appl. Phys. 80 (1996) 1099.

[37] R. Pittini, J. Schoenes, P. Wachter, Physica B 230–232 (1997) 538.

[38] J.A. Paixão, G.H. Lander, P.J. Brown, H. Nakotte, F.R. de Boer, E. Brück, J. Phys.: Condens. Matter 4 (1992) 829.

[39] J.A. Paixão, G.H. Lander, A. Delapalme, H. Nakotte, F.R. de Boer, E. Brück, Europhys. Lett. 24 (1993) 607.

[40] P.A. Veenhuizen, J.C.P. Klaasse, F.R. de Boer, V. Sechovský, L. Havela, J. Appl. Phys. 63 (1988) 3064.

[41] P. Beránková, M. Kučera, M. Matyáš, A.A. Menovsky, in: 26$^{\text{iemes}}$ Journées des Actinides, Szklarska Poreba, Poland, 1996, p. 70.

[42] J. Brunner, M. Erbudak, F. Hulliger, Solid State Commun. 38 (1981) 841.

[43] P.M. Oppeneer, M.S.S. Brooks, V.N. Antonov, T. Kraft, H. Eschrig, Phys. Rev. B 53 (1996) R10437.

[44] R. Feyerherm, A. Amato, F.N. Gygax, A. Schenck, C. Geibel, F. Steglich, N. Sato, T. Komatsubara, Phys. Rev. Lett. 73 (1994) 1849.

[45] A.T. Aldred, J. Magn. Magn. Mater. 10 (1979) 42.

[46] L. Paolasini, G.H. Lander, S.M. Shapiro, R. Caciuffo, B. Lebech, L.-P. Regnault, B. Roessli, J.-M. Fournier, Phys. Rev. B 54 (1996) 7222.

[47] B. Lebech, M. Wulff, G.H. Lander, J. Rebizant, J.C. Spirlet, A. Delapalme, J. Phys. Condens. Matter 1 (1989) 10299.

[48] O. Eriksson, M.S.S. Brooks, B. Johansson, Phys. Rev. B 41 (1990) 9087.

[49] R.D. Kirby, J.X. Shen, J.A. Woollam, D.J. Sellmyer, J. Appl. Phys. 69 (1991) 4574.

[50] J.M. Fournier, E. Pleska, J. Chiapusio, J. Rossat-Mignod, J. Rebizant, J.C. Spirlet, O. Vogt, Physica B 163 (1990) 493.

[51] P. Wachter, F. Marabelli, B. Bucher, Phys. Rev. B 43 (1991) 11136.

[52] M. Mendik, P. Wachter, J.C. Spirlet, J. Rebizant, Physica B 186–188 (1993) 678.

[53] E. Gómez Marín, PhD thesis, Grenoble, 1997.

[54] M.S.S. Brooks, J. Magn. Magn. Mater. 63–64 (1987) 649.

[55] B.R. Cooper, S.P. Lim, I. Avgin, Q.G. Sheng, D.L. Price, J. Phys. Chem. Solids 56 (1995) 1509.

[56] T. Kraft, P.M. Oppeneer, V.N. Antonov, H. Eschrig, Phys. Rev. B 52 (1995) 3561.

[57] M.S.S. Brooks, T. Gasche, B. Johansson, J. Phys. Chem. Solids 56 (1995) 1491.